LATEST-GENERATION CVD-GROWN SYNTHETIC DIAMONDS FROM APOLLO DIAMOND INC.

Wuyi Wang, Matthew S. Hall, Kyaw Soe Moe, Joshua Tower, and Thomas M. Moses

Gemological and spectroscopic properties of 43 CVD synthetic diamonds from Apollo Diamond Inc. were examined to characterize the latest generation of their CVD products. These samples, which included both faceted gems and partially polished crystals, were provided as representative examples of Apollo's 2006–2007 production. Relative to the Apollo CVD products examined in 2003, the new samples showed significant improvements in size, color, and clarity. In addition to colorless and near-colorless material, fancy orange-to-pink colors are now produced. These high-quality CVD-grown diamonds, comparable in color and clarity to natural diamonds, can be identified using a combination of gemological and spectroscopic properties.

The ability to grow high-quality diamond in the laboratory has been aggressively pursued for several decades, due to the value that diamond holds in the semiconductor, optics, and gem industries. While the growth of gem-quality single-crystal diamonds under high-pressure, high-temperature (HPHT) conditions has been intensely studied and well documented, the synthesis of single-crystal diamond by the chemical vapor deposition (CVD) technique is relatively new and has evolved rapidly over the past few years. Before 2003, the CVD technique was primarily used to grow polycrystalline diamonds of micrometer size. Badzian and Badzian (1993) reported the growth of CVD single-crystal synthetic diamond as thick as 1.2 mm; subsequently, several other groups (e.g., Doering et al., 1999; Linares and Doering, 1999) reported the CVD growth of undoped and boron-doped single-crystal diamond of approximately 1 mm thickness. Yan et al. (2004) reported the successful synthesis of "thick" nitrogen-doped free-standing single-crystal diamond using the microwave plasma CVD technique, a discovery that led to numerous new applications for this material. Since then, significant improvements in growth technique and, consequently, crystal quality have been reported (Martineau et al., 2004; Yan et al., 2004; Tallaire et al., 2005; Wang et al., 2005; Miyatake et al., 2007).

Apollo Diamond Inc. of Boston, Massachusetts, demonstrated its ability to grow single-crystal CVD synthetic diamonds of moderate gem quality several years ago (Wang et al., 2003). For the most part, the samples examined in 2003 were relatively small and of limited thickness for faceting purposes. Nearly all of these early crystals were predominantly brown with varying degrees of saturation. Colorless CVD-grown diamonds, both nitrogen doped and high purity, were also synthesized by LIMHP-CNRS in France (Achard et al., 2005; Wang et al., 2005), but the reported crystals were usually

See end of article for About the Authors and Acknowledgments.
GEMS & GEMOLOGY, Vol. 43, No. 4, pp. 294–312.

Figure 1. The latest-generation CVD synthetic diamonds produced by Apollo Diamond Inc., which are now available in the gem market, showed significant improvement in quality compared to those reported by Wang et al. in 2003. These representative samples weigh 0.24–0.67 ct. Photo by Robert Weldon.

less than 1.6 mm thick. More recent CVD products from Apollo, however, have shown substantial improvements in quality.

Apollo Diamond began to formally introduce its CVD-grown diamonds to the general public in 2007. They are currently available through Bostonian Jewelers, a Boston retailer, and via inquiries directed through the company's website at www.apollodiamond.com. Due to the potential impact that gem-quality CVD synthetic diamonds might have in the consumer market, the jewelry industry has shown great interest in developing a better understanding of these products, improvements in their quality, and their potential use in jewelry applications, as well as the ability of gem-testing laboratories to identify this material and separate it from natural diamonds. In this report, we characterize the properties of CVD synthetic diamonds produced by Apollo from 2006 to 2007 that are representative of their current generation of products (figure 1).

CVD GROWTH

The CVD method of growing diamond is very different from the well-known HPHT technique. The CVD method involves gaseous reagents—typically a small amount of methane (CH_4 as the source of carbon) in hydrogen (H_2)—in a chamber with a single-crystal diamond substrate usually with {100} orientation. More than one substrate can be placed in the reaction chamber to grow several synthetic diamond crystals simultaneously. A reaction among these components is initiated with a plasma, hot filament, or combustion flame. Carbon atoms, products of a series of chemical reactions, deposit as diamond on a substrate at relatively low temperatures (~1000°C) and low pressures (between 10 and 200 torr). The reactants, products, and reactive species are transported throughout the chamber by diffusion and convection. On the substrate surface, various reactions (adsorption, diffusion, and desorption) occur among the chemical species, leading to the deposition of synthetic diamond and, ultimately, the growth of a continuous layer of synthetic diamond. Goodwin and Butler (1997) reviewed the important features of the growth environment and critical aspects of the growth process.

MATERIALS AND METHODS

CVD Samples. For this study, Apollo Diamond provided a total of 43 CVD synthetic diamonds to the GIA Laboratory for examination; 31 were faceted, and the remainder were fashioned into cylinders or partially polished plates. The samples were segregated into three color groups: colorless to near colorless (29), fancy orange to pink (11), and dark brown (3). The entire suite ranged from 0.13 to 1.20 ct. See

TABLE 1. The three groups of latest-generation Apollo CVD-grown synthetic diamonds examined for this study.

Sample number	Shape	Cut grade[a]	Weight (ct)	Color	Clarity	Fluorescence to long-wave UV	Fluorescence to short-wave UV
Near colorless							
AP-01	Round brilliant	Very good	0.15	E	VVS_2	Inert	Inert
AP-02	Princess	na	0.30	F	VS_1	Very weak orange	Very weak orange
AP-03	Round brilliant	Very good	0.19	F	VVS_2	Inert	Inert
AP-04	Round brilliant	Very good	0.14	G	VS_1	Inert	Inert
AP-05	Round brilliant	Excellent	0.21	F	VS_1	Inert	Inert
AP-06	Round brilliant	Very good	0.16	G	VS_1	Inert	Inert
AP-07	Round brilliant	Good	0.20	I	SI_2	Inert	Very weak orange
AP-08	Round brilliant	Very good	0.27	H	VS_2	Inert	Inert
AP-09	Round brilliant	Very good	0.23	H	VVS_2	Inert	Very weak orange
AP-10	Round brilliant	Excellent	0.27	J	SI_2	Inert	Very weak orange
AP-12	Round brilliant	Very good	0.20	H	VVS_2	Inert	Inert
AP-13	Round brilliant	Good	0.21	L	VS_2	Inert	Inert
AP-14	Round brilliant	Very good	0.25	I	VS_2	Inert	Inert
AP-15	Round brilliant	Very good	0.30	I	SI_1	Inert	Inert
AP-16	Round brilliant	Good	0.25	M	VS_1	Inert	Inert
AP-17	Round brilliant	Very good	0.20	J	VVS_1	Inert	Inert
AP-18	Round brilliant	Excellent	0.62	K	I_1	Inert	Very weak orange
AP-19	Round brilliant	Good	0.28	H	VS_2	Very weak orange	Inert
AP-20	Round brilliant	Excellent	0.26	I	SI_2	Very weak orange	Very weak orange
AP-21	Cylinder	na	0.36	na	na	Inert	Inert
AP-22	Cylinder	na	0.24	na	na	Inert	Inert
AP-23	Cylinder	na	0.19	na	na	Inert	Inert
AP-24	Cylinder	na	0.31	na	na	Inert	Inert
AP-25	Cylinder	na	0.37	na	na	Inert	Inert
AP-26	Cylinder	na	0.52	na	na	Inert	Very weak orange
AP-27	Cylinder	na	0.13	na	na	Inert	Inert
AP-28	Cylinder	na	0.52	na	na	Inert	Inert
AP-29	Cylinder	na	0.32	na	na	Inert	Inert
AP-30	Cylinder	na	0.25	na	na	Inert	Inert
Orange to pink							
AP-31	Tabular	na	1.05	Brownish orangy pink	na	Weak orange, chalky	Very weak orange
AP-32	Tabular	na	1.20	Pinkish brown	na	Very weak orange	Very weak orange
AP-33	Rectangular	na	0.71	Fancy Dark brownish pinkish orange	SI_1	Weak orange, chalky	Very weak orange
AP-34	Princess	na	0.28	Fancy Dark pink-brown	VS_2	Weak orange, chalky	Very weak orange
AP-37	Round brilliant	na	0.34	Fancy brown-pink	VVS_2	Weak-to-moderate orange, chalky	Very weak orange
AP-38	Round brilliant	na	0.40	Fancy orange-brown	SI_2	Moderate orangy yellow	Weak orangy yellow
AP-39	Round brilliant	na	0.62	Fancy brown-orange	SI_2	Moderate orangy yellow	Weak orangy yellow
AP-40	Round brilliant	na	0.18	Fancy brown-pink	VVS_2	Weak orange, chalky	Weak orange
AP-41	Round brilliant	na	0.16	Fancy brown-pink	VVS_1	Weak orange, chalky	Very weak orange
AP-42	Round brilliant	na	0.58	Fancy brownish orangy pink	VVS_1	Moderate orange, chalky	Weak orange, chalky
AP-49	Round brilliant	na	0.19	Fancy brownish pink	VS_2	Weak orange, chalky	Weak orange, chalky
Dark brown							
AP-35	Round brilliant	na	0.33	Fancy Dark yellowish brown	SI_1	Inert	Inert
AP-50	Round brilliant	na	0.46	Fancy Dark orangy brown	VS_1	Inert	Inert
AP-51	Round brilliant	na	0.29	Fancy Dark orangy brown	SI_2	Inert	Inert

[a]*GIA's cut grading system applies only to colorless or near-colorless round brilliant cut diamonds. For other shapes and fancy colors, "na" (not applicable) is indicated.*

table 1 for a full description of the individual samples. These CVD-grown diamonds are representative of current Apollo Diamond production processes.

Gemological Examination. For the purpose of this study, experienced GIA diamond grading staff determined color and clarity grades on all faceted samples using the standard conditions and methodology of GIA's clarity and color grading systems (see, e.g., King et al., 1994). We examined the internal features of all the samples using both a standard gemological binocular microscope and a research microscope with a variety of lighting techniques. Reactions to ultraviolet radiation (again, see table 1) were checked in a darkened room with a conventional four-watt combination long-wave (365 nm) and short-wave (254 nm) UV lamp. We also examined all samples for their fluorescence and phosphorescence properties, as well as growth characteristics, using the Diamond Trading Company (DTC) DiamondView deep-ultraviolet (<230 nm) luminescence imaging system (Welbourn et al., 1996).

Spectroscopic Analysis. All samples were tested by all of the following methods. To avoid surface contamination in the spectroscopic analysis, we cleaned the samples thoroughly in acetone using an ultrasonic bath. Infrared absorption spectra were recorded in the mid-infrared (6000–400 cm^{-1}, 1 cm^{-1} resolution) and near-infrared (up to 11000 cm^{-1}, 4 cm^{-1} resolution) ranges at room temperature with a Thermo-Nicolet Nexus 670 Fourier-transform infrared (FTIR) spectrometer equipped with KBr and quartz beam splitters. We used a diffuse reflectance apparatus to focus the incident beam on the sample, and collected a total of 512 scans (per spectrum) to improve the signal-to-noise ratio. Spectra in the mid-infrared and near-infrared regions were normalized based on the two-phonon and three-phonon absorptions of diamond, respectively. Absorption spectra in the ultraviolet to visible to near-infrared (UV-Vis-NIR) range (250–850 nm) were recorded with a Thermo-Spectronic Unicam UV500 spectrophotometer that used a sampling interval of 0.1 nm for all samples. The synthetic diamonds were mounted in a cryogenic cell and cooled to liquid nitrogen temperature (~77 K).

Raman and photoluminescence (PL) spectra were recorded using a Renishaw InVia Raman confocal microspectrometer with an Ar-ion laser operating at two excitation wavelengths: 488 nm (for the 490–950 nm range) and 514.5 nm (for the 517–950 nm range). We collected PL spectra in the 640–850 nm range using a He-Ne laser (633 nm), and in the 835–1000 nm range using a NIR laser (830 nm). For PL analysis, all samples were cooled by direct immersion in liquid nitrogen. Three scans were accumulated to achieve a better signal-to-noise ratio.

GEMOLOGICAL OBSERVATIONS

Shapes. Most of the 31 faceted samples were round brilliants (two were princess cuts and one was a rectangular cut); they ranged in size from 0.14 to 0.71 ct. All the faceted gems exhibited standard cut dimensions. Based on the GIA cut grading system for round brilliant diamonds (Moses et al., 2004), most (14 of 18) of the colorless/near-colorless round brilliants were graded as excellent or very good.

Both ends of the 10 near-colorless cylinders were polished for quantitative spectroscopic analysis and better examination of internal features. These cylinders varied in diameter from 2.40 to 3.75 mm and in thickness from 1.51 to 2.56 mm. All displayed distinctive groove patterns on their edges, indicating that each was laser cut from a larger crystal; similar grooves were seen on the girdles of many of the faceted samples (figure 2). The two partially polished plates (1.05 and 1.20 ct) exhibited a tabular morphology (figure 3), which is characteristic of as-grown CVD synthetic diamonds.

Color. An outstanding feature of the 43 CVD-grown diamonds were the colors represented (again, see table 1). Twenty-nine samples were colorless, near colorless (figure 4), or only very slightly colored, and these are collectively referred to as the "near-colorless" group in this article. Of the 19 samples in this group given color grades (table 1; the cylinders were not color graded), four were colorless (E to F), 12 were near colorless (G to J), and three displayed very slight coloration (K to M). All the faceted Apollo samples in this group, except for the colorless ones, had a slightly brown component with no yellow apparent. Of the 14 fancy-color CVD products, 11 had significant orange or pink (or both) components with moderate-to-strong saturation (e.g., figure 5, a–c), and the other three samples were dark brown (e.g., figure 5d). Although the hue descriptions are similar between some of the samples in the "orange-to-pink" group and the three in the "dark brown" group (again, see table 1), these latter three specimens showed distinctly darker tone than the other 11 fancy-color samples and the predominant

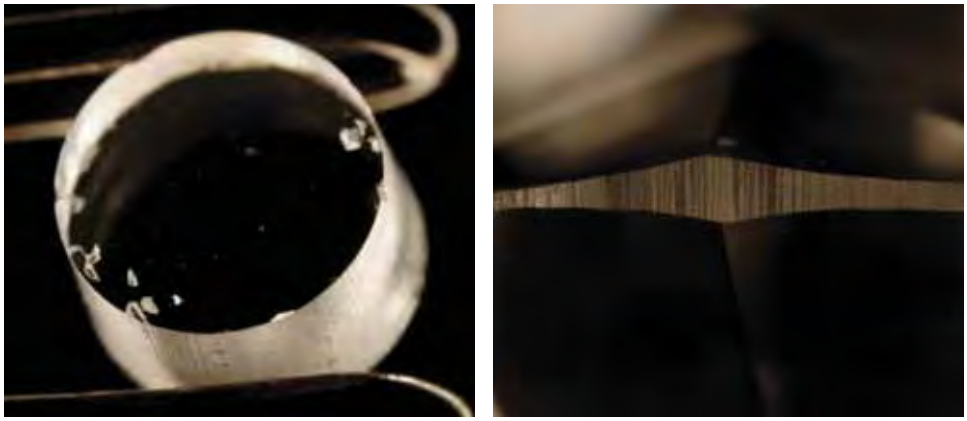

Figure 2. Most of the partially polished CVD-grown crystals examined were cylindrical with distinctive laser grooves along the outer rims. The diameter of this cylinder (left, sample AP-21) is 3.46 mm. The laser grooves were still visible on the girdles of many of the faceted round brilliants (right, sample AP-10, field of view 1.0 mm). Photomicrographs by W. Wang.

hue in all three was brown. Two samples in the "orange-to-pink" group were graded Fancy Dark, but both displayed a distinct orange-to-pink hue. Throughout this article, gemological and spectroscopic features will be presented and discussed in terms of these three color groups.

Clarity. GIA lab staff also determined clarity grades for the 31 faceted CVD-grown diamonds. Nine were given VVS grades (29%), 12 were VS (39%), and nine were SI (29%). One sample fell into the I ("included") category. Cavities, fractures, small inclusions, and pinpoints (figure 6) were the most common clarity grade–setting internal features. The fractures and cavities varied from micrometer to millimeter scale, and most were surface reaching. Unlike what is typically seen in natural diamonds, the fractures in the CVD samples were usually not connected to inclusions. In general, the small inclusions and pinpoints were randomly distributed. In rare cases, numerous pinpoints and small inclusions occurred together in cloud-like groups (figure 6c). Internal features were typically light in color with only a few small dark inclusions observed.

Reactions to UV Radiation. Observation of the samples while they were exposed to conventional short- and long-wave UV lamps revealed a close correlation between fluorescence and bodycolor (table 1). For the near-colorless group, only eight of the 29 samples showed very weak orange fluorescence to short- and/or long-wave UV radiation; the remaining samples were inert to both wavelengths. In contrast, all the samples in the orange-to-pink group showed orange fluorescence of very weak to moderate intensity to long-wave UV, with obvious turbidity ("chalkiness") in eight of the 11 samples. When exposed to short-wave UV, all of these CVD samples displayed very weak to weak orange to orangy yellow fluorescence. No UV fluorescence was observed in the three diamonds in the dark brown group. None of the samples in the present study showed phosphorescence to conventional long- or short-wave UV radiation.

When exposed to the high-intensity ultra-short wavelengths of the DTC DiamondView, most of the near-colorless group of synthetic diamonds displayed strong pinkish orange fluorescence (figure 7a and 7c), and a few fluoresced strong orange or

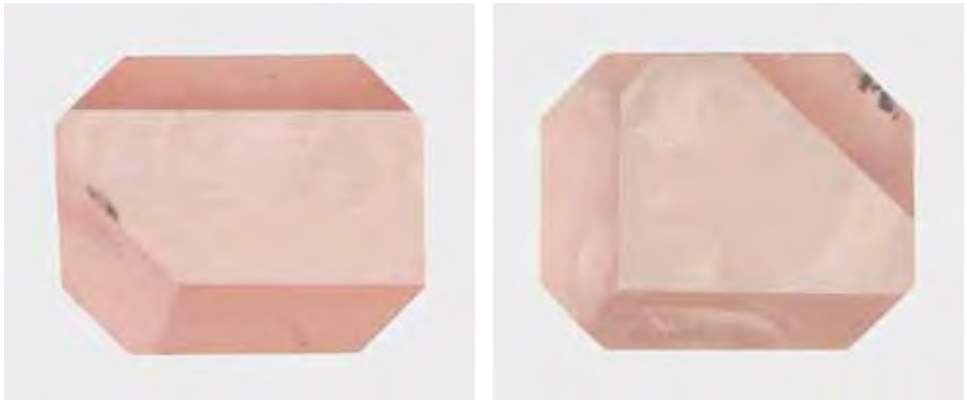

Figure 3. These two partially polished CVD crystals (1.05 and 1.20 ct) had a tabular morphology that is characteristic of CVD synthetic diamonds. Photos by Jian Xin (Jae) Liao.

Figure 4. These faceted CVD samples from Apollo Diamond (0.15–0.30 ct) range from E to H on the GIA color grading scale. Photos by Jian Xin (Jae) Liao.

orangy red (figure 7b). An interesting feature was the occurrence of regions with irregularly patterned strong blue fluorescence. The size of these regions varied significantly between samples. In some of the samples, the blue fluorescence was concentrated near the culet (figure 7c), and in others it was on the table facet. In the latter case, a violetish blue fluorescence was typically observed as well (figure 7d). All samples were also checked for phosphorescence in the DiamondView (all under the same conditions). Weak-to-moderate blue phosphorescence was seen in 15 of the 29 samples in the near-color-

Figure 5. Some of the CVD samples showed attractive fancy colors: (a) 0.71 ct, Fancy Dark brownish pinkish orange; (b) 0.34 ct, Fancy brown-pink; (c) 0.28 ct, Fancy Dark pink-brown; (d) 0.33 ct, Fancy Dark yellowish brown. Photos by Jian Xin (Jae) Liao.

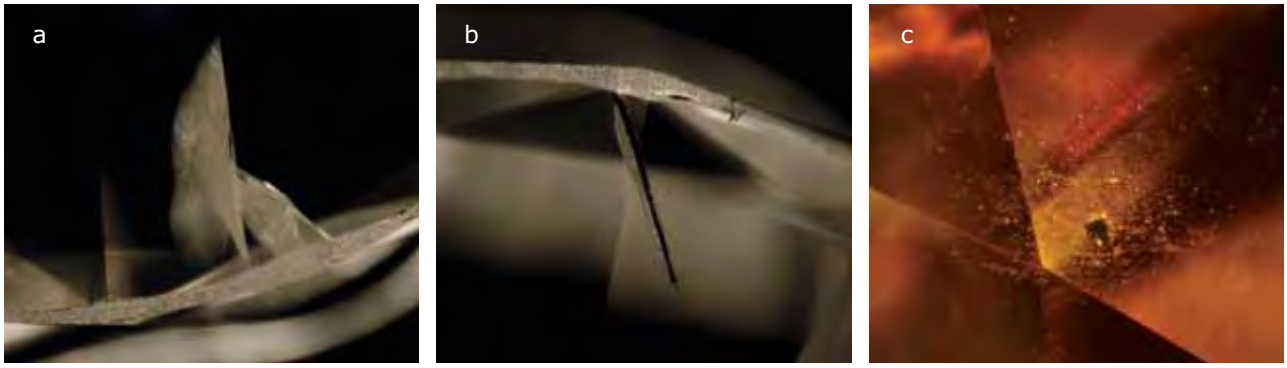

Figure 6. Most of the faceted CVD synthetic diamonds studied had high clarity grades, in the VVS and VS ranges. The internal features that most affected the clarity grades were: (a) surface-reaching fractures (field of view 2.5 mm); (b) surface-reaching cavities (field of view 1.4 mm); and (c) pinpoints and clouds (field of view 0.9 mm). Photomicrographs by W. Wang and K. S. Moe.

less group (figure 8). Within this group, we did not observe any systematic changes in fluorescence/phosphorescence in the DiamondView as the color grade increased from E to M. In general, the phosphorescence colors appeared evenly distributed throughout the CVD-grown diamonds, with no variations visible even in samples showing the distinct zonations of blue and orange-to-pink fluorescence.

The orange-to-pink CVD synthetic diamonds showed stronger reddish orange fluorescence in the DiamondView (figure 9a-d) than was seen in the near-colorless samples; none showed the irregularly patterned blue fluorescence. In general, the fluorescence in the orange-to-pink samples was evenly distributed, with only three of the 11 samples showing bands of weaker orange color. These bands were uniform in thickness, oriented parallel to the table facet, and had sharp, well-defined boundaries (figure

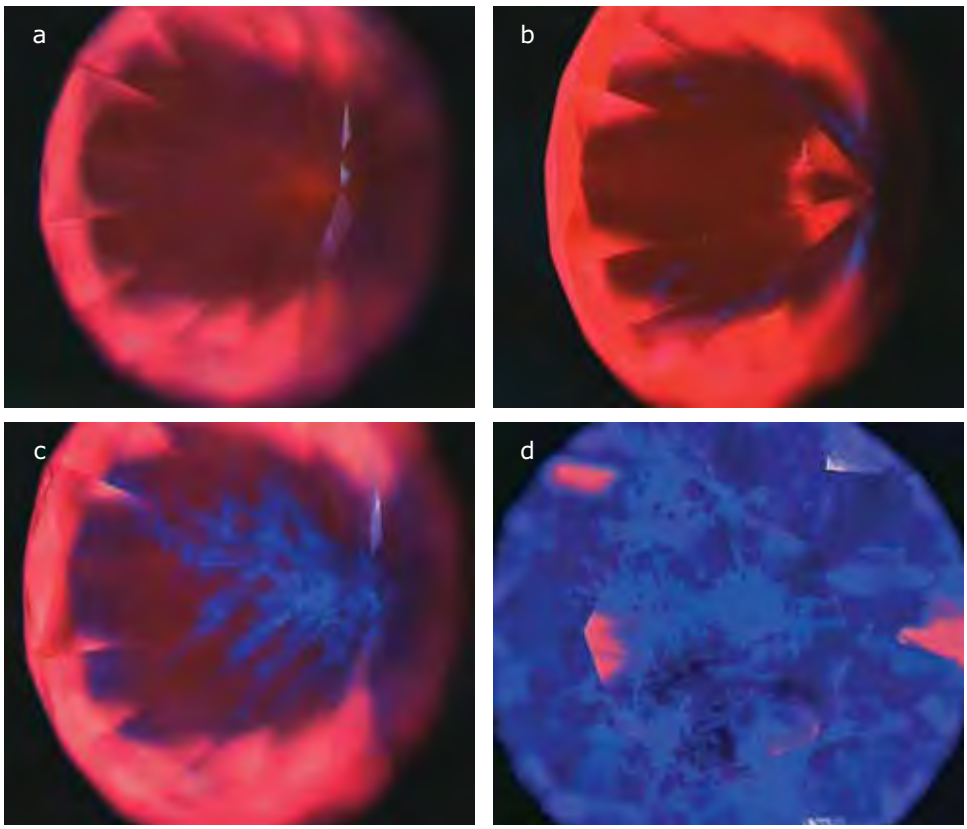

Figure 7. In the DTC DiamondView, most of the near-colorless group of CVD synthetic diamonds displayed strong pinkish orange fluorescence (a and c), and some fluoresced strong orange or orangy red (b). Several had very irregular regions with strong blue (c) or violetish blue (d) fluorescence. Photos by W. Wang.

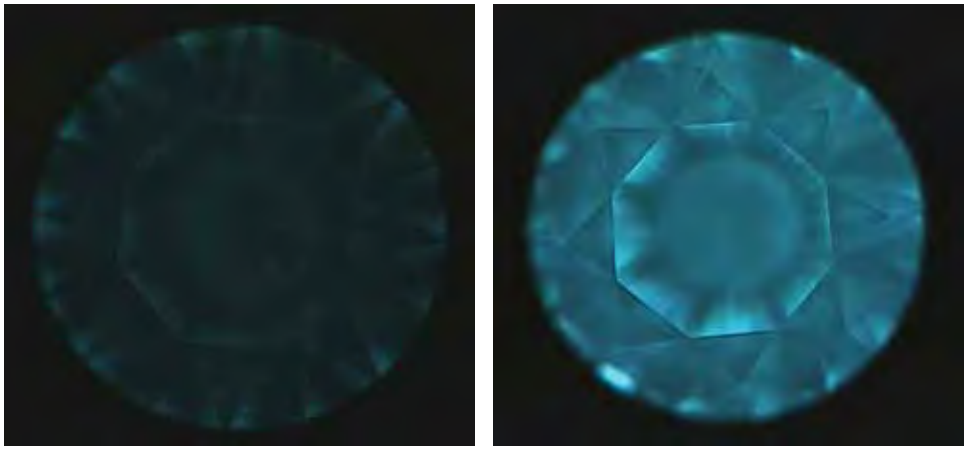

Figure 8. The DiamondView revealed blue phosphorescence of weak (left) to moderate (right) intensity in about half of the CVD-grown diamonds in the near-colorless group. All the phosphorescence images were collected under the same conditions. Photos by W. Wang and K. S. Moe.

9b). Narrow growth striations were visible in many of the samples due to variations in fluorescence intensity, and evenly distributed weak green fluorescence (figure 9c) was also observed in five of the 11 orange-to-pink samples. Of all the fancy-color CVD synthetic diamonds studied, only one of the orange-to-pink samples (AP-34) showed weak blue plus some small areas of green phosphorescence (figure 10) in the DiamondView.

The three dark brown CVD synthetic diamonds showed orangy red fluorescence in the DiamondView, but with much weaker intensity than that of the other two groups. The irregularly patterned blue fluorescence observed in the near-colorless group also occurred in the brown samples, but was very limited in distribution.

Graining and Birefringence. Graining was a common feature in all the CVD synthetic diamonds studied. In contrast to that observed in natural dia-

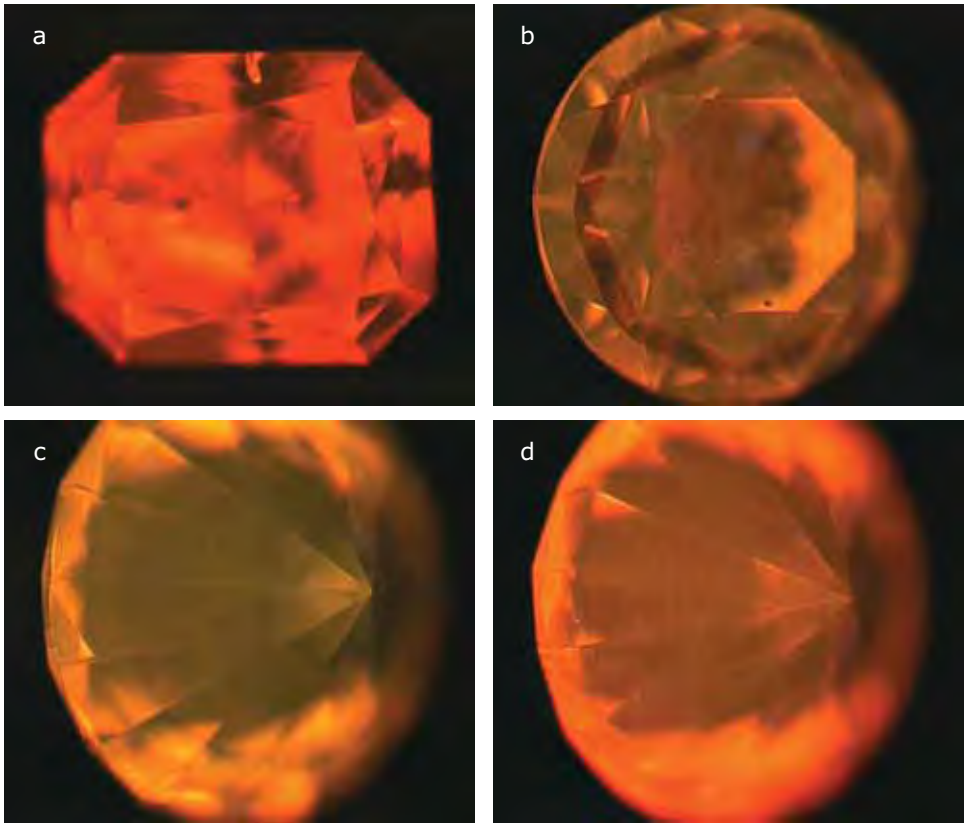

Figure 9. The fancy-color CVD synthetic diamonds with distinct orange-to-pink colors showed a more intense reddish orange fluorescence (a–d) than the near-colorless group when examined with the DiamondView. Three of the 11 samples in this group showed bands of weaker orange fluorescence (b), possibly due to variations in crystal growth conditions. Five also displayed distinct green fluorescence (c). Photos by W. Wang and K. S. Moe.

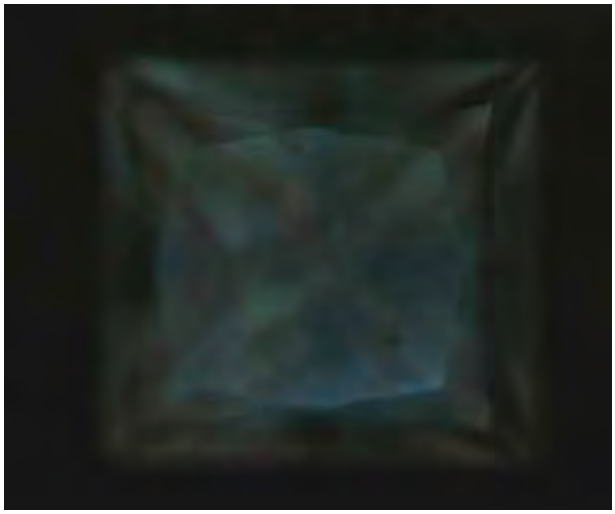

Figure 10. Only one (AP-34) of the 14 fancy-color CVD-grown diamonds phosphoresced in the DiamondView, showing weak blue with minor amounts of green luminescence. Photo by W. Wang.

Figure 11. Internal graining was well developed but "fuzzy" in most of the CVD synthetic diamonds studied. Graining with clearly observable outlines, as seen here in sample AP-18, was rare. Photomicrograph by W. Wang; field of view 2.4 mm.

monds, the internal graining in most of the CVD samples showed indistinct boundaries that appeared fuzzy. Only three samples showed graining with relatively well-defined edges (see, e.g., figure 11).

Strong birefringence was another important feature of these CVD samples. Under magnification with crossed polarizers, all the samples displayed very high-order interference colors (figure 12). The CVD products commonly showed red, blue, green, and even white interference colors that were in sharp contrast to the gray colors that are typical of natural type IIa diamonds. While bands of interference colors occurred in a few samples, most displayed irregular patterns. No correlation was observed between bodycolor and interference color or pattern; comparable interference features occurred in both the near-colorless and fancy-color CVD groups.

RESULTS OF SPECTROSCOPIC ANALYSIS

Infrared Absorption Spectroscopy. Several distinct features in the IR spectra correlated directly with the bodycolors of the CVD synthetic diamonds. In the mid-infrared region, samples in the near-colorless group showed no detectable absorptions related to nitrogen or boron impurities, indicating they

Figure 12. When examined with crossed polarizers, type IIa CVD synthetic diamonds usually show much higher-order interference colors than natural type IIa diamonds, as illustrated by the samples shown here: (a) type IIa faceted CVD-grown diamond; (b) type IIa cylindrical CVD-grown crystal; and (c) interference pattern of a typical natural type IIa diamond. Photomicrographs (fields of view 1.8, 3.8, and 1.4 mm, respectively) by W. Wang and K. S. Moe.

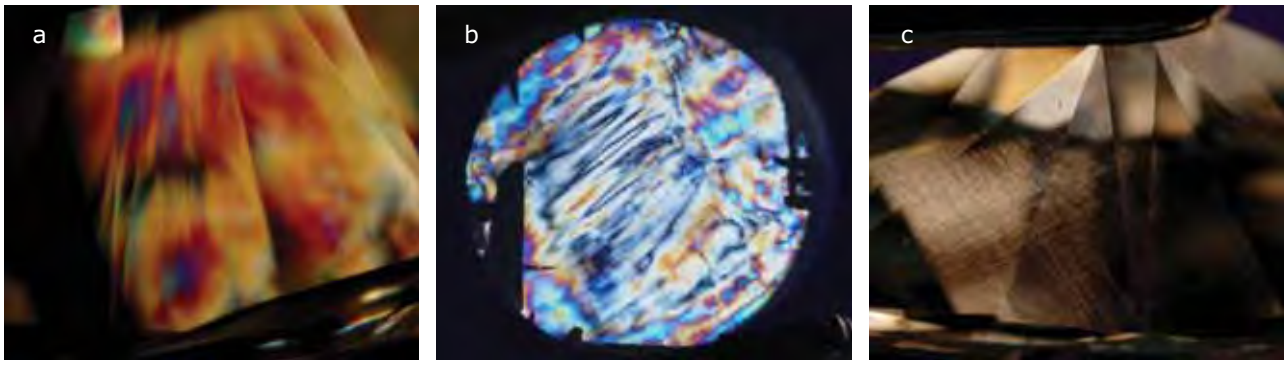

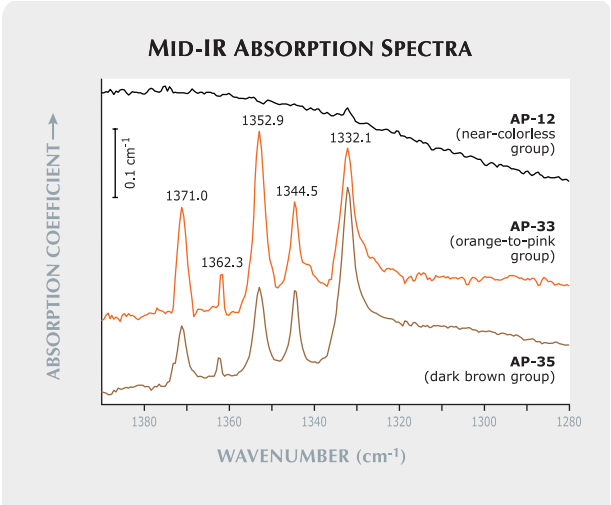

Figure 13. CVD synthetic diamonds from the near-colorless group (e.g., AP-12) showed only a weak absorption at 1332.1 cm^{-1}. In the fancy-color CVD diamonds (e.g., AP-33, AP-35), more intense peaks were observed. Spectra shifted vertically for clarity.

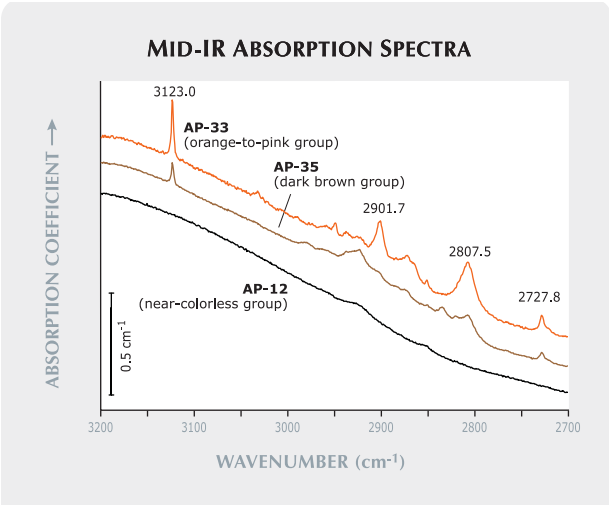

Figure 14. In the near-colorless group of CVD synthetic diamonds (e.g., AP-12), no absorption at 3123.0 cm^{-1} was recorded. In contrast, that H-related absorption is very strong in the fancy-color CVD diamonds (e.g., AP-33, AP-35). Spectra shifted vertically for clarity.

were all type IIa, and exhibited only a weak peak at 1332.1 cm^{-1} (figure 13). All the fancy-color samples showed stronger absorption at 1332.1 cm^{-1}. Additionally, all were classified as type IIa; however, they showed a weak absorption at 1344.5 cm^{-1} (~0.1 cm^{-1} in intensity) that was due to the presence of ~5 ppm of isolated nitrogen. In addition, weak but distinct absorptions at 1371.0, 1362.3, and 1352.9 cm^{-1} were consistently recorded in the fancy-color CVD-grown diamonds, but did not occur in the near-colorless group.

Differences between the near-colorless and fancy-color samples were also noted in the region of 3200–2700 cm^{-1} (figure 14). In this range, CVD samples in the near-colorless group showed only the gradual increase in absorption that is intrinsic to diamond. In contrast, all the fancy-color samples exhibited a sharp absorption at 3123.0 cm^{-1} with significant intensity caused by a hydrogen-related lattice defect (Fuchs et al., 1995a,b). Many other weak and broad features also occurred in this region, including peaks at 2901.7, 2807.5, and 2727.8 cm^{-1}.

The integrated intensities of the absorptions (i.e., the areas under the peaks) at 1371.0 and 1352.9 cm^{-1}, as represented in figure 13, displayed positive linear correlations with each other (figure 15, left; a similar correlation for the 1362.3 peak is not shown) and with the H-related peak at 3123.0 cm^{-1} (figure 15, right), but no correlation was observed with the concentration of isolated nitrogen (i.e., the 1344.5 cm^{-1} peak).

We also observed significant variations in the near-infrared range (figure 16). For the near-colorless CVD group, the samples ranging in color from F to J showed only two very weak absorptions at 6855 and 5562 cm^{-1}, whereas the E-color sample (AP-01) had no detectable absorptions in the entire NIR region. The K-to-M CVD synthetic diamonds generally showed two additional weak absorptions at 7353 and 6425 cm^{-1}. While all of these absorptions were <1.0 cm^{-2} in integrated intensity, NIR features in the K-to-M samples appeared slightly stronger than those in samples from the rest of the near-colorless group.

The orange-to-pink CVD samples exhibited much stronger absorptions at 7353 (average integrated intensity 2.12 cm^{-2}) and 6425 cm^{-1}. However, they did not show the peaks at 6855 and 5562 cm^{-1}; instead, many sharp peaks occurred in the range 9000–4200 cm^{-1}, including the strong absorptions at 7917 and 7804 cm^{-1} reported by Twitchen et al. (2007) as the 1263 and 1281 nm lines. This group of samples showed other major NIR peaks at 7533, 6963, 6828, 6425, 6064, 5219, 4888, 4672, and 4337 cm^{-1} (again, see figure 16, left). All the lines were sharp and relatively strong in intensity.

The three dark brown CVD synthetic diamonds showed absorption features that were very similar to those of the K-to-M colors, with two additional sharp and strong peaks at 8752 and 7837 cm^{-1}, and two sharp peaks at 7225 and 7189 cm^{-1} (figure 16, right). In these three dark brown diamonds, all the peaks were very strong and linearly correlated with

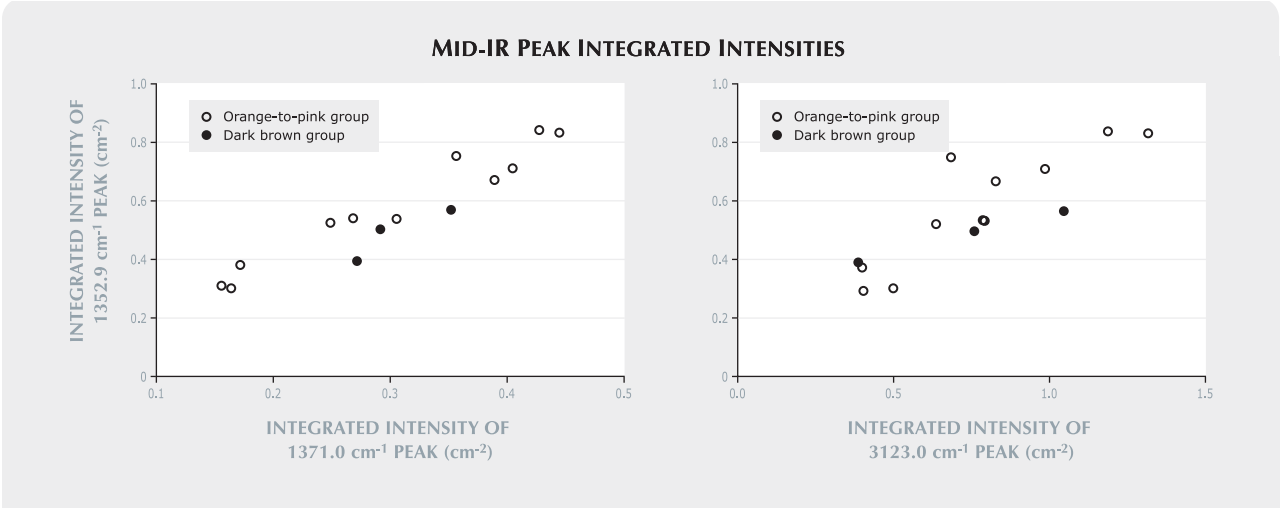

Figure 15. In the fancy-color CVD synthetic diamonds, the integrated intensities displayed positive linear correlations between (left) absorptions at 1352.9 cm^{-1} and 1371.0 cm^{-1}, and (right) those absorptions (represented here by the peak at 1352.9 cm^{-1}) and the H-related absorption at 3123.0 cm^{-1}.

one another in integrated intensity (figure 17). For example, the average integrated intensity of the 7353 cm^{-1} peak in the dark brown samples was 89.2 cm^{-2}.

UV-Vis-NIR Absorption Spectroscopy. The E-to-J CVD-grown diamonds in the near-colorless group showed no specific features in the UV-Vis region except for a very slight increase in absorption from ~500 nm to the high-energy (low-wavelength) side (e.g., sample AP-22 in figure 18). An extremely weak and broad band at ~270 nm was recorded in the slightly brown samples. Sample AP-16, which had the most brown ("M") in the near-colorless group, also had the highest-intensity absorption at ~270 nm of the near-colorless samples. The broad ~270 nm band is caused by trace amounts of isolated nitrogen.

Analysis of the samples in the orange-to-pink group revealed some consistent absorption features, including broad bands at ~270 nm and ~520 nm, a gradual increase in absorption from ~450 nm to the

Figure 16. Some distinct correlations were observed between absorptions in the near-infrared region and the body-colors of the CVD samples. Generally, the orange-to-pink samples (e.g., AP-33) showed stronger peaks than those in the near-colorless group (e.g., AP-04 and AP-13; left). In dark brown CVD diamonds (e.g., AP-51; right), very strong absorptions were consistently observed. Note the difference in scale between the spectra on the left and right; also, spectra on the left have been shifted vertically for clarity.

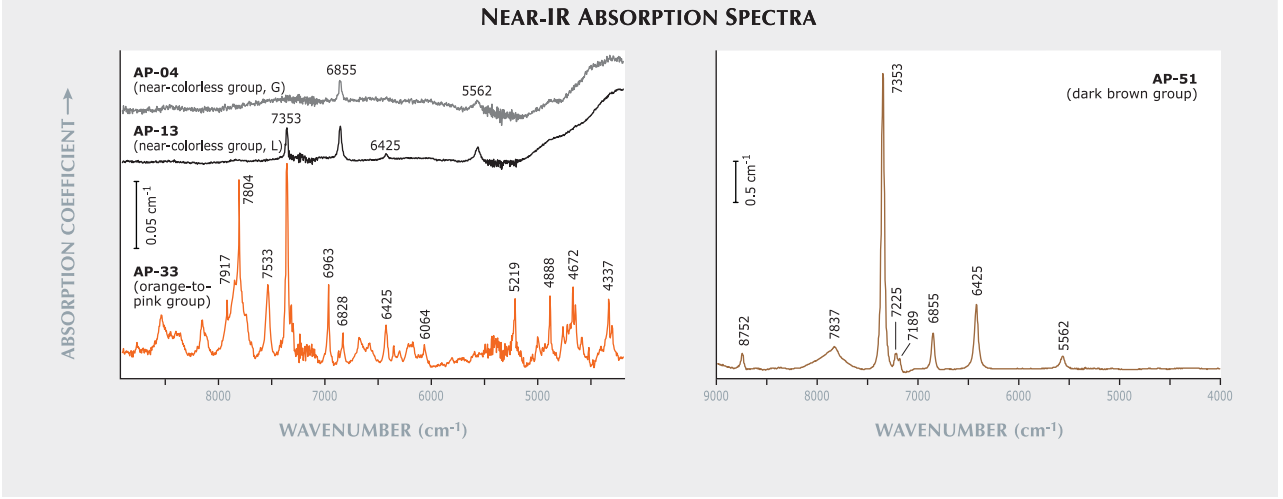

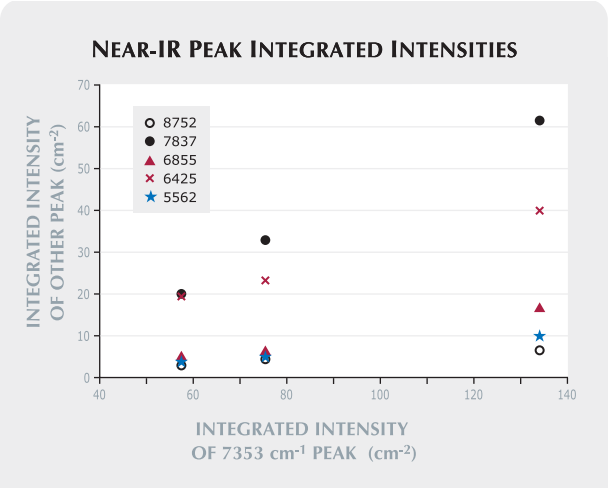

Figure 17. Six absorption peaks in the near-infrared region of the dark brown CVD synthetic diamonds displayed positive linear correlations.

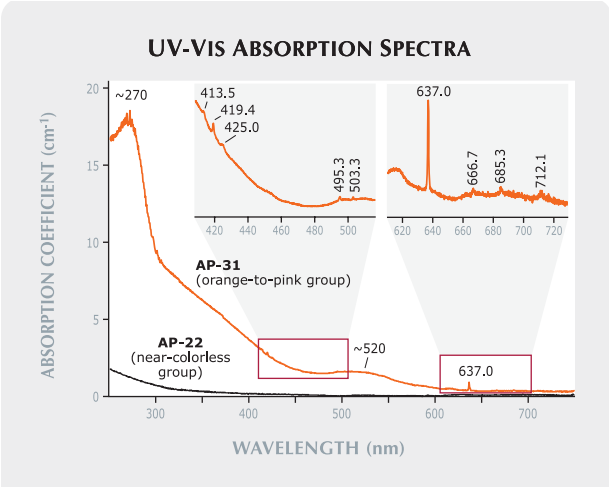

Figure 18. In the UV-Vis region, absorption spectra from CVD samples of the near-colorless group (e.g., AP-22) are generally flat. Broad bands at ~270 nm and ~520 nm and some sharp peaks including a ZPL at 637.0 nm were consistently recorded in CVD samples with orange-to-pink coloration (e.g., AP-31).

high-energy (low-wavelength) side, and sharp peaks at 413.5, 419.4, 425.0, 495.3, 503.3, 637.0, 666.7, 685.3, and 712.1 nm (see spectrum of sample AP-31 in figure 18). Among the sharp absorptions, the 637.0 nm peak, the zero phonon line (ZPL) of the nitrogen-vacancy $[N\text{-}V]^-$ center, was the strongest. In the three dark brown samples, absorption increased gradually from ~600 nm to the high-energy (low-wavelength) side with a broad band centered at ~520 nm (figure 19). Only two sharp, but weak, absorptions at 624.5 and 637.6 nm were recorded. A broad shoulder centered at ~370 nm appeared in samples AP-35 and AP-50; however, the feature is difficult to discern in sample AP-51 due to very strong absorption in this region. All these broad features are similar to those reported in as-grown brown CVD synthetic diamond by, for example, Martineau et al. (2004, figure 11), Twitchen et al. (2004, 2007), and Hounsome et al. (2005).

Photoluminescence and Raman Spectroscopy. Numerous emission lines were recorded with four different lasers, some of which were observed with multiple excitation wavelengths. The major PL features are summarized below on the basis of individual laser excitation in the defect's most sensitive region.

When blue laser (488 nm) excitation was employed (figure 20), all the CVD synthetic diamonds in the near-colorless group displayed weak and sharp peaks at 543.3 and 546.1 nm. Weak peaks at 501.2, 534.0, 534.4, and 540.0 nm also occurred in over 70% of the samples in this group (not shown); in general, these weak peaks were either all present or all absent. A weak emission at 512.2 nm (not shown) was also observed in about half the samples tested. An outstanding feature in the near-colorless group was the occurrence of a weak 3H emission (ZPL at 503.5 nm) in about 70% of the samples. Only one sample (AP-14) showed a very weak H3 emission (ZPL at 503.1 nm). All the orange-to-pink CVD samples showed extremely strong H3 emissions as well as a cluster of weak emissions at 493.7–500.9 nm with major lines at 494.6, 498.1 (not shown), and 546.1 nm. Moderate H3 emissions

Figure 19. This absorption spectrum is typical of the dark brown CVD synthetic diamonds.

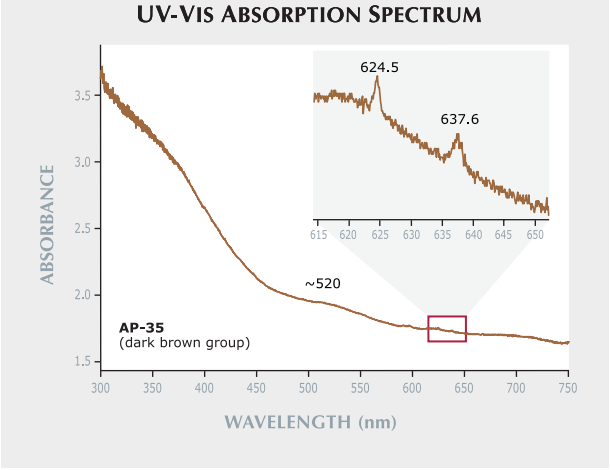

were also recorded in all three dark brown CVD samples, together with a 512.2 nm peak (not shown). Additional weak emissions at 540.0 (not shown), 543.3, and 546.1 nm were present in some of the samples of this group.

Green laser (514.5 nm) excitation revealed strong emission systems of N-V centers in the CVD samples of all colors (575 and 637.0 nm [not shown]; figure 21). Doublet emissions at 596.5 and 597.0 nm occurred in all samples of the near-colorless group. The same doublet appeared in all three dark brown samples, but with an additional weak peak at 595.3 nm. In contrast, these features were absent in the orange-to-pink CVD synthetic diamonds. In addition, all three dark brown samples exhibited weak peaks, as shown in the inset to figure 21, at 555.0, 557.1, and 559.1 nm, with the strongest intensity at 559.1 nm. These correspond to Raman shifts at 1418, 1486, and 1550 cm^{-1}, respectively. The last of these is due to the presence of non-diamond carbon (Zaitsev, 2001). The Raman shifts of these three peaks were confirmed based on the same energy shift (i.e., these features appeared at different wavelengths, but with the same Raman shift, when excited by the two different lasers) using 488 nm laser excitation but with weaker intensity than those obtained from 514.5 nm laser excitation.

When excited by a red laser (633 nm), all the samples in the near-colorless group showed weak silicon-related emission (figure 22), which is usually composed of two very sharp peaks at 736.6 and 736.9 nm (generally referred to as the 737 nm defect; Vavilov et al., 1980; Clark et al., 1995; Iakoubovskii et al., 2001). We should point out that this emission also was present in 75% of the samples of this group when 488 or 514.5 nm laser excitation was used. In addition, weak emissions at 664.0, 665.8, and 833.8 nm (not shown) were recorded with the red laser in about half the samples in the near-colorless group. In all the orange-to-pink samples, a weak emission occurred at 823.4 nm. However, the Si-related 737 nm emission was observed in eight of the 11 samples. While most Si-related emissions were very weak in this group, two samples (AP-38 [figure 22] and AP-39) displayed extremely strong peaks. None of the orange-to-pink samples showed Si-related emission peaks when 488 or 514.5 nm laser excitation was used. Of the three dark brown CVD synthetic diamonds, only one (AP-50) showed a very weak emission at the Si-related 737 nm defect (again, see figure 22). No emission at 737 nm was observed in the other two dark brown samples with any laser excitation.

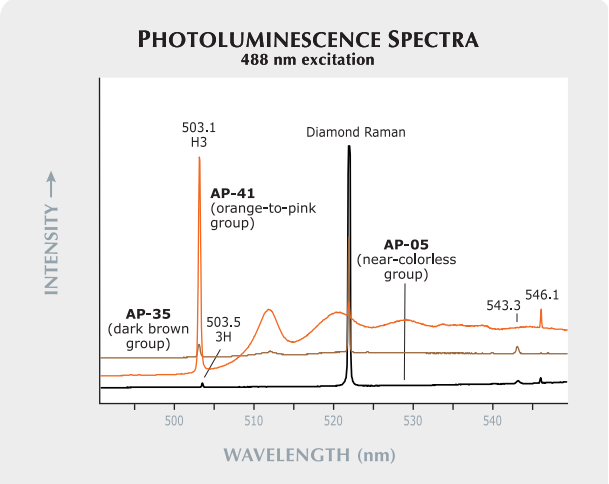

Figure 20. When blue laser (488 nm) excitation was used, the PL spectra showed H3 emission in the orange-to-pink (e.g., AP-41) and dark brown (e.g., AP-35) CVD samples. A weak 3H emission occurred in most of the CVD samples in the near-colorless group (e.g., AP-05). Other peaks, such as at 543.3 and 546.1 nm, were also observed among the various color groups.

Infrared laser excitation at 830 nm produced many weak and sharp emission features in the

Figure 21. The PL spectra of all CVD synthetic diamonds examined in this study were dominated by N-V center emission systems at 575 nm (the 637 nm peak is not shown) when green laser (514.5 nm) excitation was employed. In addition, Raman scattering peaks at 1418, 1486, and 1550 cm^{-1} (555.0, 557.1, and 559.1 nm) were observed in all three dark brown CVD synthetic diamonds (inset) but not in any sample of other colors.

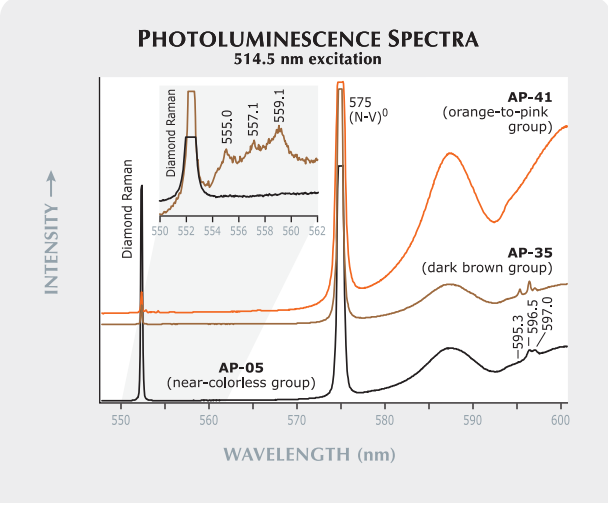

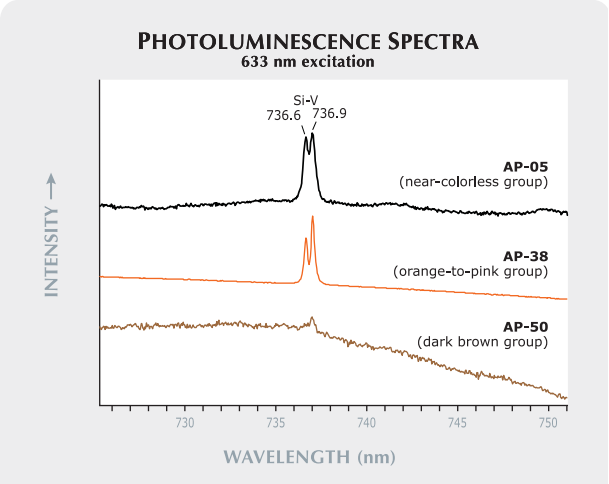

Figure 22. Si-related emission peaks at 736.6 and 736.9 nm were recorded with varying intensities in the PL spectra of most CVD synthetic diamonds. These features were best seen when red laser excitation at 633 nm was used.

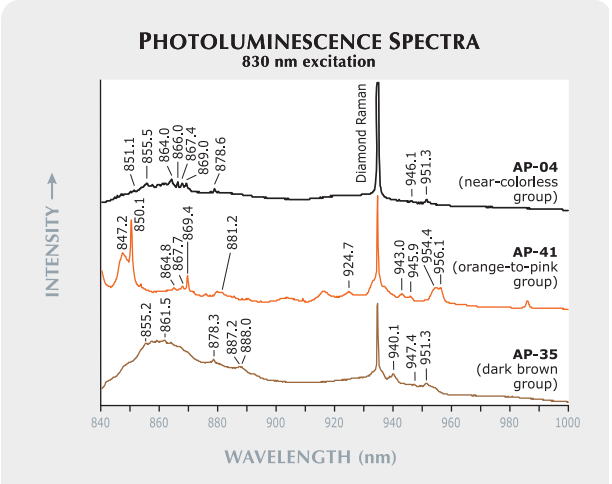

Figure 23. Many weak emission lines were detected in the infrared region of the PL spectra when 830 nm laser excitation was used. Clear differences were observed among the near-colorless, orange-to-pink, and dark brown CVD samples.

850–880 nm region for the near-colorless group of CVD-grown diamonds, including peaks at 851.1, 855.5, 864.0, 866.0, 867.4, 869.0, and 878.6 nm (figure 23). We also observed weak peaks at 946.1 and 951.3 nm in all samples of this group. In the orange-to-pink CVD-grown diamonds, we recorded even more weak emissions, including those at 847.2, 850.1, 864.8, 867.7, 869.4, 881.2, 924.7, 943.0, 945.9, 954.4, and 956.1 nm. The dark brown CVD samples exhibited fewer emissions, among them weak peaks at 855.2, 861.5, 878.3, 887.2, 888.0, 940.1, 947.4, and 951.3 nm.

DISCUSSION

Improvements in Gem Quality. As previously reported (Wang et al., 2003), gem-quality synthetic diamonds grown by Apollo Diamond Inc. represented some of the first examples of single-crystal material grown by the CVD process that were intended for the jewelry trade. Most of the samples produced at the time that article was published showed limited thickness due to the tabular morphology of the CVD crystal. For the most part, the few faceted synthetic diamonds studied were a very strong brown, relatively small (<0.30 ct), and received moderate-to-low clarity grades (VS_1–SI_2). In comparison, the 2006–2007 Apollo Diamond products showed substantial improvements in color, with colorless, near-colorless, and fancy orange-to-pink material representative of the gem-quality CVD-grown diamonds that are now commercially available.

In addition to the previously documented near-colorless and brown CVD material, Martineau et al. (2004) reported on high-quality single-crystal CVD synthetic diamond with blue color produced by boron doping during crystal growth and on a 0.85 ct round-cut as-grown fancy brownish pink CVD synthetic diamond (see sample N8 in table 3 of that reference). Until the present article, little was known about the gemological and spectroscopic features of orange-to-pink CVD synthetic diamonds produced by Apollo Diamond. These very attractive colors, as shown in figures 1 and 5, are comparable to some top-quality fancy-color natural diamonds.

Improvements in clarity were also observed. The clarity grades of over 67% of the samples provided from Apollo's recent production fell in the range VVS_1–VS_2. Only a few were in the SI–I range. Improved clarity was mainly achieved by reducing the amount of larger inclusions and pinpoints. While most of the samples examined for this study contained some pinpoints, very few contained other inclusions that could be resolved even under magnification up to 100×. However, several fractures were observed, particularly in the samples fashioned as cylinders. Significant internal stress was indicated by strong birefringence in many specimens (figure 12). As with natural diamonds, internal stress in these CVD synthetic diamonds—or the stress of the cutting process—is likely to contribute to cracking. Improvements in the CVD growth process have led to larger faceted gems. Even though most of the faceted gems in the current study were still under

0.30 ct, the fact that many samples over half a carat were available and that those cut as round brilliants were well proportioned (table 1) indicates that thicker crystals are used to create the latest-generation Apollo products. In brief, the overall color and clarity of the CVD synthetic diamonds examined in this study is similar to that of the Element Six CVD products reported by Martineau et al. (2004).

It should be noted, though, that the CVD synthetic diamonds examined by Martineau et al. are not commercially available. Apollo products similar in quality to those described in this report have been introduced to the gem trade. All of these CVD-grown products carry a distinctive inscription that identifies them as Apollo Diamonds.

Causes of Improved Clarity and Color. Production of top-quality CVD synthetic diamonds using a relatively high growth rate continues to be a challenge, leading to extensive testing of various combinations of growth parameters. Achard et al. (2005) reported that incorporating as little as 10 ppm of nitrogen in the total gas phase could increase the crystal growth rate by a factor of 2.5 with no degradation of the surface morphology or color. However, Achard et al.'s samples were not of gem thickness, so the color could not be graded using accepted gemological techniques.

According to Martineau et al. (2004), based on growth conditions and additional treatment after growth, CVD synthetic diamonds may be divided into four groups, including high purity and nitrogen doped. The nitrogen-doped product contains a detectable amount of N-bearing lattice defects in UV-Vis absorption and/or photoluminescence spectroscopy, whereas high-purity samples do not. The occurrence of N-V centers, observed as very strong emission systems in the PL spectra of all the Apollo CVD samples tested for the present study (figure 21), indicated that all the samples contained nitrogen. Even in the colorless (E and F) CVD samples, emission from the N-V centers was readily detectable. However, there is a strong correlation between increasing color and greater N-V emission (normalized to the Raman peak height). This is further evidence that nitrogen plays a leading role in the determination of color in the CVD-grown diamonds.

The reasons for nitrogen doping in these CVD samples were different for each color group. For the near-colorless group, nitrogen was controlled at relatively low levels to achieve high growth rates while maintaining crystal quality (Linares and Doering, 2003). IR absorption spectroscopy did not detect any nitrogen impurities in samples of this group. However, the extremely weak, broad band seen at ~270 nm in the UV-Vis-NIR absorption spectra of the samples with a slightly brownish hue is due to isolated nitrogen in concentrations at the ppm (parts per million) level. Non-diamond carbon, deposited during CVD diamond growth, is known to cause brown color in CVD synthetic diamonds; however, the absence of non-diamond carbon (figure 21), and the weak correlation between the concentration of isolated nitrogen and the color grades, suggests that the slight brownish hue in near-colorless samples could be caused by a combination of the detected defects such as isolated nitrogen and N-V centers; additionally, non-diamond carbon could be present, but in concentrations too low to be detected with Raman spectroscopy.

The impact of nitrogen doping in the fancy-color CVD synthetic diamonds is more complicated. Higher concentrations of nitrogen were added into the gas phase and, as a result, more nitrogen was incorporated into the diamond lattice during growth. Relatively high concentrations of isolated nitrogen were revealed in the IR and UV-Vis-NIR absorption spectra (figures 13 and 18). Only 5 ppm of isolated nitrogen is needed to produce yellow-to-orange color in diamond. Moderately strong absorption from the $[N\text{-}V]^-$ defect (ZPL at 637.0 nm; figure 18) in combination with the broad ~520 nm band likely resulted in selective absorption of orange light, and produced a pink color. Assignment of the ~520 nm broad band is unclear, but in these samples it functioned very similarly to the ~550 nm broad absorption band known to cause the color in many natural pink diamonds by selectively absorbing green-to-orange light. The ~520 nm broad band could have been the main color contributor for this group of diamonds.

The dark brown diamonds are distinctive due to the presence of non-diamond carbon (figure 21), which was not detected in either of the other two CVD groups studied. The combination of relatively high concentrations of isolated nitrogen, a weak-to-moderate absorption band at ~520 nm, and the presence of non-diamond carbon resulted in a gradual increase in absorption from the low-energy to high-energy (high-wavelength to low-wavelength) side of the UV-Vis-NIR absorption spectra. Consequently, brown coloration was produced in these samples.

Defect Interrelations and Their Implications. Absorptions with varying intensities at 3123.0,

1371.0, 1362.3, and 1352.9 cm^{-1} occurred in the fancy-color CVD samples (again, see figures 13 and 14). The 3123.0 cm^{-1} absorption is routinely observed in nitrogen-doped single-crystal CVD synthetic diamonds (Wang et al., 2003; Martineau et al., 2004). The absorption was studied via isotopic substitution with ^2D (i.e., deuterium, isotope of hydrogen with mass 2 amu) and determined to be a vibration involving a single hydrogen atom (Fuchs et al., 1995b). Recent investigation of the 3123.0 cm^{-1} absorption using a combination of annealing and uniaxial-stress experiments suggested that the NVH^- defect is responsible (Cruddace et al., 2007a).

The negative nitrogen-vacancy-hydrogen complex, NVH^-, was first identified in single-crystal CVD synthetic diamond using electron paramagnetic resonance (EPR) spectroscopy (Glover et al., 2003). Hydrogen is a common IR-active impurity in natural type Ia and occasionally type IIa diamonds, often showing a sharp absorption at 3107 cm^{-1}. Chrenko et al. (1967) first found this absorption, and Woods and Collins (1983) proposed that it originated from a C-H stretching vibration mode.

The variation in peak positions of hydrogen-related absorption is one of the most important spectroscopic differences between natural and CVD synthetic diamonds. Positive correlations in intensity among all these four peaks (figure 15) indicated that the other three peaks (1371.0, 1362.3, and 1352.9 cm^{-1}) could also be related to or caused by the NVH^- defect. Meanwhile, recent studies (Cruddace et al., 2007a,b) using uniaxial-stress experiments revealed different symmetries of these centers. These discrepancies are not fully understood. Based on the relationship Cruddace et al. (2007a) established, we calculated that the concentrations of NVH^- defect varied from 1.3 to 4.3 ppb in these fancy-color CVD synthetic diamonds.

Many of the peaks in the near-infrared region (8752, 7353, 6855, 6425, and 5562 cm^{-1}; figure 16) were reported in Wang et al. (2003). These peaks were present in the near-colorless and dark brown samples, but with an additional one at 7837 cm^{-1}. Interstitial hydrogen and hydrogen trapped at vacancies are potential candidates for the absorption at 7353 cm^{-1} (Goss, 2003). In the dark brown samples, these absorptions were extremely strong, which permitted accurate determination of their integrated intensities and thus allowed us to investigate their correlations. Similar positive linear correlations also occurred among six absorption peaks (8752, 7837, 7353, 6855, 6425, and 5562 cm^{-1}) in the near-infrared region (figure 17), but none of these peaks showed any observable correlation with the 3123.0 cm^{-1} absorption in intensity. All these observations indicate that the six absorption peaks in the near-IR region of the dark brown samples are very likely related to or caused by the same defect, but not the NVH^- defect.

An outstanding feature of the PL spectrum of the orange-to-pink CVD-grown diamonds is the strong H3 center (figure 20). The occurrence of H3 is reinforced by the green fluorescence (figure 9c). The H3 defect is in the neutral charge state $(N\text{-}V\text{-}N)^0$. This defect forms in nitrogen-bearing diamonds through combination of the nitrogen A aggregate and a vacancy. Formation of this defect usually involves irradiation and annealing at relatively high temperatures (e.g., Collins, 1982, 2001) or is associated with distinct plastic deformation features. While very common in irradiated/annealed type Ia diamonds, varying concentrations of the H3 defect also occur in some natural-color type Ia diamonds. The H3 defect can be a major contributor to the yellow color in some natural diamonds (King et al., 2005). In natural type IIa diamonds, though, the H3 defect is observed in extremely low concentrations or is not detectable even when very sensitive PL spectroscopy is employed. Strong H3 emissions, as observed in the PL spectra of the orange-to-pink CVD samples in this study, are extremely rare in natural type IIa diamonds, as well as in CVD synthetic diamonds of other colors. The occurrence of relatively high concentrations of the H3 defect in this specific group indicates a possible link to the production of orange-to-pink hues.

The 3H defect that was observed in most diamonds in the near-colorless group is widely believed to be introduced by radiation and has a complicated annealing behavior. Heating to 300–400°C may increase the 3H center intensity considerably depending on the concentration of nitrogen in the diamond (Zaitsev, 2001). This defect can be stable at temperature as high as 1000°C (Steeds et al., 1999). Most CVD diamond growth occurs at ≥800°C and it is more likely that the 3H center was introduced during the crystal growth process.

Twitchen et al. (2007) first reported the development of 7917 and 7804 cm^{-1} absorptions in the near-infrared region (corresponding to the 1263 and 1281 nm peaks in the reference) in CVD synthetic diamonds when annealed to 1400–1500°C at ambient pressure. In a recent uniaxial stress and annealing study, Cruddace et al. (2007c) further found that

the 7354 cm^{-1} system annealed out in the temperature range of 1300–1600°C at ambient pressure, and two lines at 7917 and 7804 cm^{-1} appeared. These two peaks, as well as many others, were observed in all the Apollo fancy orange-to-pink samples with varying intensities (figure 16).

In addition, features similar to those seen in prior research were observed in the UV-Vis-NIR absorption spectra. Weak absorption peaks at 503.3 (due to H3 defects) and 666.7 nm (figure 18) in their orange-to-pink CVD synthetic diamonds developed when brown CVD synthetic diamond was annealed (Twitchen et al., 2007). The absorption feature at approximately 624 nm disappeared when their sample was heated in the range of 1200–1400°C (Twitchen et al., 2007). In the present study, a feature at 624.5 nm was seen in the spectra of the dark brown samples (figure 19) but not in those of the orange-to-pink group. The mechanism for the occurrence of the spectroscopic features observed with IR/UV-Vis-NIR absorption and PL spectroscopy in the orange-to-pink CVD synthetic diamonds studied for the present report is not well understood, and further investigation is ongoing.

Identification Features. The progress made over the past few years toward the efficient growth of single-crystal CVD synthetic diamond has opened a range of possible industrial and jewelry applications (figure 24). Several other organizations and institutes (e.g., Element Six, Carnegie Institute, LIMHP-CNRS in France, and the National Institute for Material Sciences in Japan) have demonstrated the capability to grow single-crystal CVD diamond with products of varying sizes and quality. In addition, Apollo Diamond Inc. has begun producing and marketing CVD-grown gems to the jewelry industry.

Identification and separation of CVD synthetic diamonds from natural diamonds can be achieved through careful attention to the gemological and spectroscopic properties. While not conclusive, several gemological observations serve as good indications of CVD material: strong internal graining with an indistinct "fuzzy" appearance, high-order interference colors (figure 12a), occurrence of pinpoints and occasional clouds (figure 6), and remnant laser grooves on the girdles (figure 2b). These gemological features do, however, appear in some natural diamonds (Moses et al., 1999). Crystal inclusions are not commonly present in either CVD or natural type IIa diamonds, but when they are present, their appearance can be diagnostic of natural origin.

Early products from Apollo with varying saturations of brown color displayed a weak orange fluorescence to UV radiation that was considered a useful indication of CVD synthesis (Wang et al., 2003; Martineau et al., 2004). However, this feature is absent from most of the new products due to improvements in the growth technique and crystal quality. Most of the samples in the near-colorless and dark brown groups were inert, and only a few near-colorless samples showed very weak orange fluorescence under the UV lamp. The very weak to moderate orange fluorescence observed in the orange-to-pink samples, on the other hand, was similar to that seen in some natural pink diamonds (King et al., 2002), which also makes this property problematic as an identification criterion.

Fluorescence and phosphorescence images obtained from the DTC DiamondView continue to be very useful for identification of CVD synthetic diamonds. Orange fluorescence with irregularly patterned areas of blue fluorescence, narrow growth bands, and blue phosphorescence (figures 7–9) appear to be characteristic features of CVD-grown diamonds, if present. Most natural type IIa diamonds show relatively uniform blue fluorescence and rarely show phosphorescence in the DiamondView. Although a few natural type IIa diamonds show orange fluorescence, the co-existence of orange and irregular blue fluorescent regions has not been observed in natural stones. In addition, natural type IIa diamonds often show characteristic internal features (e.g., "mosaic" networks of polygonized dislocations) that likely would not occur in CVD synthetic diamonds. Natural diamonds with trace amounts of isolated nitrogen rarely show any pink hue, or dominant red-orange fluorescence in the DiamondView.

Spectroscopic features are very important for CVD identification. For near-colorless samples, the occurrence of weak absorptions in the near-infrared region (7353, 6855, 6425, 5562 cm^{-1}; figure 16) and/or a very weak absorption band at ~270 nm in the UV-Vis-NIR region are indicative of CVD growth. Occurrence of a 3123.0 cm^{-1} absorption in the mid-infrared region was considered to be an important feature of the early CVD synthetic diamonds (Wang et al., 2003), but this absorption was absent in all of the near-colorless group tested. Important identification features from photoluminescence spectroscopy (figures 20–23) include strong emissions from N-V centers, the 596/597 doublet, and emissions at 534.0, 543.3, 546.1, 736.6,

Figure 24. CVD lab-grown diamonds are now available in fine jewelry, such as these stackable rings set in yellow and white gold. Courtesy of Apollo Diamond Inc.

736.9, 946.1, and 951.3 nm. These luminescence features can be activated by lasers of various wavelengths. Occurrence of the 3H defect in most of the near-colorless group of CVD samples (figure 20) is not well understood, and this feature has also been reported in CVD synthetic diamonds from another producer (Wang et al., 2005).

Many of the previously listed emissions (596/597 doublet, and emissions at 534.0, 543.3, 546.1, 736.6, 736.9, 946.1, and 951.3 nm) are specific to CVD synthetic diamonds and have not been detected in natural diamonds (Martineau et al., 2004; Wang et al., 2005). However, it should be pointed out that the Si-related 737 nm emission was recently found in natural type IIa and low-nitrogen diamonds (Breeding et al., 2007). Since the Si-related 737 nm emission is extremely rare in natural diamonds, its occurrence in photoluminescence spectroscopy is still a very useful indicator of a CVD synthetic diamond.

For those CVD synthetic diamonds with orange-to-pink and dark brown colors, IR absorption spectroscopy proved more useful for identification than photoluminescence. Occurrence of a sharp 3123.0 cm^{-1} absorption (figure 14) from an H-related defect and the combination of absorptions at 1371.0, 1362.3, 1352.9, and 1344.5 (due to isolated nitrogen) are specific to these fancy-color CVD synthetic diamonds (figure 13). Very strong absorptions at 8752, 7837, 7353, 6855, 6425, and 5562 cm^{-1} in dark brown samples and numerous (7917, 7804, 7533, 7353, 6963, 6828, 6425, 6064, 5219, 4888, 4672, and 4337 cm^{-1}) sharp absorption peaks in the near-infrared region of orange-to-pink samples (figure 16) are characteristic identification features for these two groups. The ~520 nm broad absorption band in UV-Vis-NIR spectra (figures 18 and 19) is slightly lower in position than the 550 nm band in natural diamonds. The well-known 596/597 photoluminescence doublet emissions were entirely absent in the orange-to-pink CVD synthetic diamonds, and the Si-related 737 nm emission occurred in few of the fancy-color CVD-grown diamonds.

The identification of CVD synthetic diamonds from natural stones may be achieved based on a combination of various gemological and spectroscopic features. There is no single feature that will ensure proper identification of all CVD synthetic diamonds, and testing in a properly equipped gemological laboratory is needed to guarantee confident identification.

CONCLUSIONS

Compared to earlier-generation products, the CVD synthetic diamonds submitted by Apollo Diamond Inc. as representative of their 2006–2007 production showed significant improvements in color and clarity. Relatively larger, well-proportioned, faceted CVD products have also become more common. Colorless, near-colorless, and attractive fancy-color material is now being produced. The new products are comparable in quality to many natural diamonds in the marketplace. The gem sizes (0.14–0.71 ct) reflect the highest-volume segment of the natural diamond market. These CVD synthetic diamonds exhibited unusual internal graining, high birefringence, complex fluorescence zoning, and several distinct spectroscopic features. All of these CVD synthetic diamonds can be identified, but a combination of various gemological and, especially, spectroscopic features is required to do so consistently and accurately. We anticipate that CVD diamond growth techniques will continue to improve and CVD products with even better quality will eventually be introduced to the gem market.

ABOUT THE AUTHORS
Dr. Wang (wuyi.wang@gia.edu) is manager of research projects, Mr. Hall is manager of identification services, Mr. Moe is research technician, and Mr. Moses is senior vice president, at the GIA Laboratory, New York. Mr. Tower is senior scientist at Apollo Diamond Inc., Boston, Massachusetts.

ACKNOWLEDGMENTS
The authors thank Ivana Balov, Thomas Gelb, Joshua Cohn, Paul Johnson, Dino DeGhionno, Shane McClure, Dr. James Shigley, Dr. Andy H. Shen, and Dr. Christopher M. Breeding of the GIA Laboratory for their many suggestions and assistance in this study. Dr. Robert Linares, Patrick Doering, and their team at Apollo Diamond are specially thanked for their continued cooperation with GIA and for their efforts to cooperate with the jewelry industry to develop a better understanding of CVD diamond growth technology. Constructive reviews by Dr. John Angus, Dr. James Butler, Dr. Philip Martineau, and Dr. Christopher Welbourn helped improve this article substantially.

REFERENCES

Achard J., Tallaire A., Sussmann R., Silva F., Gicquel A. (2005) The control of growth parameters in the synthesis of high-quality single crystalline diamond by CVD. *Journal of Crystal Growth*, Vol. 284, No. 3/4, pp. 396–405.

Badzian A., Badzian T. (1993) Diamond homoepitaxy by chemical vapor deposition. *Diamond and Related Materials*, Vol. 2, No. 2/4, pp. 147–157.

Breeding C.M., Wang W. (2007) Occurrence of the Si-V (737 nm) center in a natural type IIa colorless gem diamond. *Abstract of 18th European Conference on Diamond, Diamond-like Materials, Carbon Nanotubes, and Nitride.* Berlin, Germany, September 9–14 , p. P1.04.04.

Chrenko R.M., McDonald R.S., Darrow K.A. (1967) Infrared spectra of diamond coat. *Nature*, Vol. 213, No. 5075, pp. 474–476.

Clark C.D., Kanda H., Kiflawi I., Sittas G. (1995) Silicon defects in diamond. *Physical Review B*, Vol. 51, No. 23, pp. 16681–16688.

Collins A.T. (1982) Colour centers in diamond. *Journal of Gemmology*, Vol. 18, No. 1, pp. 35–75.

Collins A.T. (2001) Colour of diamond and how it may be changed. *Journal of Gemmology*, Vol. 27, No. 6, pp. 341–359.

Cruddace R.C., Newton M.E., Smith H.E., Davies G., Martineau P.M., Twitchen D.J. (2007a) Identification of the 3123 cm^{-1} absorption line in SC-CVD diamond as the NVH^- defect. *Proceedings of the 58th De Beers Diamond Conference*, Coventry, England, pp. 15.1–15.3.

Cruddace R.C., Newton M.E., Smith H.E., Davies G., Fisher D., Martineau P.M., Twitchen D.J. (2007b) Uniaxial stress and annealing measurements on C-H bands in diamond. *Proceedings of the 58th De Beers Diamond Conference*, Coventry, England, pp. P19.1–P19.3.

Cruddace R.C., Newton M.E., Davies G., Martineau P.M., Twitchen D.J. (2007c) Uniaxial stress and annealing studies of the NIR 913 meV system in SC-CVD diamond. *Proceedings of the 58th De Beers Diamond Conference*, Coventry, England, pp. P20.1–P20.2.

Doering P.J., Linares R.C. (1999) Large area single crystal CVD diamond: Properties and applications. *Proceedings of Applied Diamond Conference / Frontier Carbon Technology Joint Conference 1999*, Tsukuba, Japan, pp. 32–35.

Fuchs F., Wild C., Schwarz K., Muller-Sebert W., Koidl P. (1995a) Hydrogen induced vibrational and electronic transitions in chemical vapor deposited diamond, identified by isotopic substitution. *Applied Physics Letters*, Vol. 66, No. 2, pp. 177–179.

Fuchs F., Wild C., Schwarz K., Koidl P. (1995b) Hydrogen-related IR absorption in chemical vapour deposited diamond. *Diamond and Related Materials*, Vol. 4, No. 5/6, pp. 652–656.

Goss J.P. (2003) Theory of hydrogen in diamond. *Journal of Physics: Condensed Matter*, Vol. 15, No. 17, pp. R551–R580.

Glover C., Newton M.E., Martineau P.M., Twitchen D.J., Baker L.M. (2003) Hydrogen incorporation in diamond: The nitrogen-vacancy-hydrogen complex. *Physical Review Letters*, Vol. 90, No. 18, pp. 185507–185510.

Goodwin D.G., Butler J.E. (1997) Theory of diamond chemical vapor deposition. In M.A. Prelas, G. Popovici, and L.K. Bigelow, Eds., *Handbook of Industrial Diamonds and Diamond Films*, Marcel Dekker, New York, pp. 527–581.

Hounsome L.S., Jones R., Martineau P.M., Shaw M.J., Briddon P.R., Öberg S., Blumenau A.T., Fujita N. (2005) Optical properties of vacancy related defects in diamond. *Physica Status Solidi (a)*, Vol. 202, No. 11, pp. 2182–2187.

Iakoubovskii K., Adriaenssens G.J., Dogadkin N.N., Shiryaev A.A. (2001) Optical characterization of some irradiation-induced centers in diamond. *Diamond and Related Materials*, Vol. 10, No. 1, pp. 18–26.

King J.M., Moses T.M., Shigley J.E., Liu Y. (1994) Color grading of colored diamonds at the GIA Gem Trade Laboratory. *Gems & Gemology*, Vol. 30, No. 4, pp. 220–242.

King J.M., Shigley J.E., Guhin S.S., Gelb T.H., Hall M. (2002) Characterization and grading of natural-color pink diamonds. *Gems & Gemology*, Vol. 38, No. 2, pp. 128–147.

King J.M., Shigley J.E., Gelb T.H., Guhin S.S., Hall M., Wang W. (2005) Characterization and grading of natural-color yellow diamonds. *Gems & Gemology*, Vol. 41, No. 2, pp. 88–115.

Linares R.C., Doering P.J. (1999) Properties of large single crystal diamond. *Diamond and Related Materials*, Vol. 8, No. 2/5, pp. 909–915.

Linares R.C., Doering P.J. (2003) *System and method for producing synthetic diamond.* US Patent 6,582,513.

Martineau P.M., Lawson S.C., Taylor A.J., Quinn S.J., Evans D.J.F., Crowder M.J. (2004) Identification of synthetic diamond grown using chemical vapor deposition (CVD). *Gems & Gemology*, Vol. 40, No. 1, pp. 2–25.

Miyatake H., Arima K., Maida O., Teraji T., Ito Y. (2007) Further improvement in high crystalline quality of homoepitaxial CVD diamond. *Diamond and Related Materials*, Vol. 16, No. 4/7, pp. 679–684.

Moses T.M., Shigley J.E., McClure S.F., Koivula J.I., Van Daele M. (1999) Observations on GE-processed diamonds: A photographic record. *Gems & Gemology*, Vol. 35, No. 3, pp. 14–22.

Moses T.M., Johnson M.L., Green B., Blodgett T., Cino K., Geurts R.H., Gilbertson A.M., Hemphill T.S., King J.M., Komylak L., Reinitz I.M., Shigley J.E. (2004) A foundation for grading the overall cut quality of round brilliant cut diamonds. *Gems & Gemology*, Vol. 40, No. 3, pp. 202–228.

Steeds J.W., Davis T.J., Charles S.J., Hayes J.M., Butler J.E. (1999) 3H luminescence in electron-radiated diamond samples and its relationship to self-interstitials. *Diamond and Related Materials*, Vol. 8, No. 10, pp. 1847–1852.

Tallaire A., Achard J., Sussmann R.S., Silva F., Gicquel A. (2005) Homoepitaxial deposition of high-quality thick diamond films: Effect of growth parameters. *Diamond and Related Materials*, Vol. 14, No. 3/7, pp. 249–254.

Twitchen D.J., Martineau P.M., Scarsbrook G.A., Dorn S.C., Cooper M.A. (2004) *Coloured diamond.* Patent publication number US2004194690.

Twitchen D.J., Martineau P.M., Scarsbrook G.A. (2007) *Coloured diamond.* Patent publication number US2007079752.

Vavilov V.S., Gippius A.A., Zaitsev A.M., Deryagin B.V., Spitsyn B.V., Aleksenko A.E. (1980) Investigation of the cathodoluminescence of epitaxial diamond films. *Soviet Physics-Semiconductors*, Vol. 14, pp. 1078–1079.

Wang W., Moses T., Linares R., Shigley J.E., Hall M., Butler J.E. (2003) Gem-quality synthetic diamonds grown by the chemical vapor deposition method. *Gems & Gemology*, Vol. 39, No. 4, pp. 268–283.

Wang W., Tallarie A., Hall M.S., Moses T.M., Achard J., Sussmann R.S., Gicquel A. (2005) Experimental CVD synthetic diamonds from LIMHP-CNRS, France. *Gems & Gemology*, Vol. 41, No. 3, pp. 234–244.

Welbourn C.M., Cooper M., Spear P.M. (1996) De Beers natural versus synthetic diamond verification instruments. *Gems & Gemology*, Vol. 32, No. 3, pp. 156–169.

Woods G.S., Collins A.T. (1983) Infrared absorption spectra of hydrogen complexes in type I diamonds. *Journal of Physics and Chemistry of Solids*, Vol. 44, No. 5, pp. 471–475.

Yan C.-S., Mao H.-K., Li W., Qian J., Zhao Y.S., Hemley R.J. (2004) Ultrahard diamond single crystals from chemical vapor deposition. *Physica Status Solidi, Rapid Research Note*, Vol. 201, No. 4, pp. R25–R27.

Zaitsev A.M. (2001) *Optical Properties of Diamond*. Springer-Verlag, Berlin, 502 pp.